

Photocycle features of heterologously expressed and assembled eukaryotic flavin-binding BLUF domains of photoactivated adenylyl cyclase (PAC), a blue-light receptor in *Euglena gracilis*

Shinji Ito,^{a,b} Akio Murakami,^c Kyosuke Sato,^d Yasuzo Nishina,^d Kiyoshi Shiga,^d Tetsuo Takahashi,^e Shoichi Higashi,^b Mineo Iseki^{b,f} and Masakatsu Watanabe^{*a,b}

^a Department of Photoscience, School of Advanced Sciences, Graduate University for Advanced Studies (SOKENDAI), Shonan Village, Hayama, Kanagawa 240-0193, Japan.

E-mail: watanabe_masakatsu@soken.ac.jp; Fax: +81-46-858-1544; Tel: +81-46-858-1561

^b National Institute for Basic Biology, National Institutes of Natural Sciences, Okazaki, Aichi 444-8585, Japan

^c Kobe University Research Center for Inland Seas, Iwaya, Awaji, Hyogo 656-2401, Japan

^d Department of Molecular Physiology, Graduate School of Medical Sciences, Kumamoto University, Honjo, Kumamoto, Kumamoto, 860-8556, Japan

^e School of Pharmaceutical Sciences, Toho University, Miyama, Funabashi, Chiba 274-8510, Japan

^f PRESTO, Japan Science and Technology Agency, Honcho, Kawaguchi, Saitama 332-0012, Japan

Received 26th April 2005, Accepted 19th July 2005

First published as an Advance Article on the web 8th August 2005

Photoactivated adenylyl cyclase (PAC) is a recently discovered blue-light photoreceptor that mediates photomovement in *Euglena gracilis* (Iseki *et al.*, *Nature*, 2002, **415**, 1047–1051). PAC appears to be a heterotetramer composed of two FAD-binding subunits (PAC α and PAC β). Both subunits have a pair of homologous regions (F1 and F2) which show homology with prokaryotic “sensors of blue-light using FAD” (BLUF) domains. The F1 and F2 domains of PAC are the only eukaryotic BLUF domains found thus far. We obtained soluble recombinant F1 and F2 proteins in PAC α by heterologous expression with fused glutathione-*S*-transferase (GST) in *E. coli*. The expressed F1 samples did not bind flavins, but the F2 samples contained both FAD and FMN with trace amounts of riboflavin. We also assembled the histidine-tagged recombinant F2 (6His-F2) from inclusion bodies in *E. coli* with exogenous FAD or FMN. Blue-light-induced changes in absorption spectra of these assembled samples were highly similar to those reported for prokaryotic BLUF domains. The FAD- or FMN-assembled 6His-F2 photocyced with nearly the same rate constants of light-reaction and dark-relaxation, which were slightly lower than those of GST-cleaved F2. The estimated quantum efficiency for the phototransformation was 0.28–0.32, and the half-life was 34–44 s at 25 °C for the recombinant PAC α F2, whereas that reported for prokaryotic BLUF domains varied from *ca.* 3.5 s (Tl10078) to *ca.* 900 s (AppA). The mutated recombinant Y472F and Q514G of PAC α F2 and the F2 domain of the PAC α homologue from *Eutreptiella gymnastica*, which lacks the Gln residue conserved in other BLUF domains, showed no photoinduced transformation.

Introduction

The photosynthetic flagellate *Euglena gracilis* uses flagellar-mediated photomovements to locate optimal light conditions for photosynthesis. Photoactivated adenylyl cyclase (PAC), which acts as a blue light regulated adenylyl cyclase, has been previously extracted from the paraflagellar bodies (PFBs) near the base of the flagella, and identified as the blue-light photoreceptor which mediates the step-up photophobic response (turning of the cell in response to abrupt increases in light intensity), resulting in avoidance from intense illumination.^{1,2} PAC noncovalently binds flavin adenine dinucleotides (FAD), and is composed of two subunits (PAC α and PAC β) which are similar to each other. Both subunits have a pair of homologous regions (F1 and F2) showing also homology with prokaryotic BLUF domains.³ F1 and/or F2 appear to be FAD-binding domains which sense blue light using FAD. It is possible that a phot signal captured in F1 and/or F2 is transferred to a catalytic domain (probably C1 and/or C2) through a conformational change, consequently elevating adenylyl cyclase activity. Other euglenoids have orthologues of PAC α and PAC β with

homologous domains of F1 and F2.⁴ These BLUF homologues constitute the only cases found so far in eukaryotic organisms.

AppA, which has a single BLUF domain,⁵ is another blue-light photoreceptor that functions as an antirepressor of photosynthetic gene expression in the purple bacterium *Rhodobacter sphaeroides*.^{6,8} A recombinant BLUF domain of AppA produced by expression in *Escherichia coli* displays a photocycle, formation of a signaling state by irradiation of blue light followed by dark regeneration of its original state, resulting in a red-shift of the absorption spectrum.^{6–13} Slr1694, which has a single BLUF domain, is probably involved in positive phototaxis in *Synechocystis* sp. PCC 6803.¹⁴ This recombinant BLUF domain shows a similar photocycle to that of AppA.¹⁵ Recently, ultrafast spectroscopic analysis of the recombinant BLUF domain of AppA and another cyanobacterial BLUF domain (Tl10078) showed that the signaling state is formed from the light-excited state within 10 ns.^{13,16}

Site-directed mutagenesis in the BLUF domains of AppA and Slr1694 suggests that a tyrosine residue conserved in all BLUF domains (at the 21st position in AppA or at the 8th position in Slr1694) is involved in the photocycle,^{7,9,17} either through

π - π stacking interaction with the isoalloxazine ring of FAD⁷ or through proton transfer from FAD.^{9,10} Spectrochemical analysis revealed that light excitation leads to structural rearrangements of the protein moieties coupled with conformational changes of the isoalloxazine rings II and III of FAD, due to hydrogen bonding.^{12,15,17,18} The recently determined crystal structures of BLUF domains of AppA and Tll0078 showed that the Tyr21 in AppA and Tyr8 in Tll0078 are hydrogen bound to Gln63 and Gln50, respectively, and each of them directly interacts with FAD by forming a hydrogen bond with O4 of isoalloxazine ring III of FAD.^{19,20} Replacement of Gln50 with Ala in Tll0078 has the same effect as the Y8F mutant, *i.e.*, suppression of the light-induced absorption changes.¹⁹

The mechanism of photoactivation of PAC is of great interest because of the regulatory interaction of the flavin binding domain with the adenylyl cyclase catalytic domain. Characterization of the putative photocycle during the photochemical reaction of PAC should provide important information about the mechanism. However, it has been difficult to obtain enough amounts of PAC or its BLUF domains (F1 and/or F2) to study their photocycle spectrophotometrically, either by large-scale purification from PFBs or by heterologous expression. During the experiments reported in this paper we obtained sufficient amounts of soluble recombinant PAC α F1 and F2 proteins fused with glutathione-S-transferase (GST) by heterologous expression in *E. coli*. The F2 samples contained both FAD and FMN with trace amounts of riboflavin.²¹ Although it is assumed that native PAC α F1 binds FAD, the expressed F1 samples did not bind flavins. In addition, we developed a method for assembly of His-tagged recombinant PAC α F2 heterologously expressed in *E. coli* and obtained from inclusion bodies. Taking advantage of these recombinant F2 samples, we examined the basic photocycling characteristics using blue LED or HeCd laser excitation and dual-wavelength spectrophotometry. Here we discuss the photocycling characteristics of a recombinant eukaryotic BLUF domain, PAC α F2, as compared to prokaryotic BLUF domains.

Because Tyr472 and Gln514 in PAC α F2 correspond to Tyr21 in AppA or Tyr8 in Slr1694, and Gln63 in AppA or Gln50 in Tll0078, required for the photocycle,^{7,9,17,19,20} we made point-mutated recombinants (Y472F and Q514G mutants) proteins fused with GST. Furthermore, the F2 domain of the PAC α homologue of *Eutroptiella gymnastica* (EtgPAC1)⁴ lacks the Gln522 residue conserved in other PAC homologues and other BLUF domains. We heterologously expressed EtgPAC1 in *E. coli* and the above described three samples were used to examine whether the Tyr and the Gln residues in eukaryotic BLUF domains are essential for the photocycle, as in the prokaryotic BLUF domains.

Materials and methods

Construction of expression vectors

Recombinant PAC α F2 was overexpressed as an N-terminal fusion with GST in *E. coli* using a tac promoter-based expression system, as shown in Fig. 1. To construct the expression plasmid, the region from Gly462 to Asp574 of PAC α , which includes the F2 domain, was amplified using the polymerase chain reaction (PCR) with a DNA polymerase (Pyrobest, Takara, Ohtsu, Japan). Forward and reverse primers, 5'-ATGGGATCCGGTGGTGAAGGCCAG-3' and 5'-CGTCGACTAGTCCTGCAGGGGTGG-3', were used to amplify the F2 coding sequence, adding *Bam*HI and *Sal*I restriction sites and a stop codon. A cloned cDNA encoding PAC α was used as a PCR template. The PCR-amplified fragment was cloned into *Bam*HI-*Sal*I restriction sites of pGEX-6P-2 (Amersham Bioscience, Piscataway, NJ, USA), resulting in recombinant plasmid pGEX-F2 for expression of the GST-fused F2 protein (GST-F2).

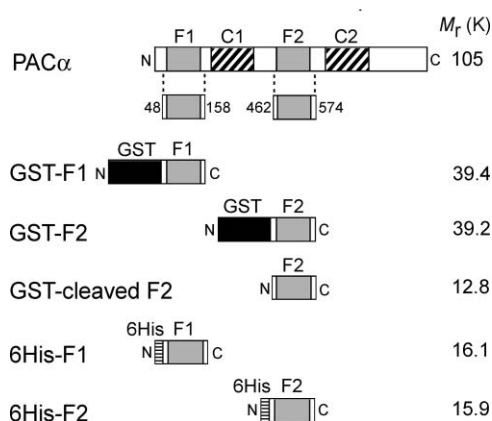


Fig. 1 Schematic structures of native PAC α and recombinant PAC α F1 and F2. Relative molecular masses (M_r) of GST-F1, GST-F2, GST-cleaved F2, 6His-F1, and 6His-F2 were calculated with the PeptideSort in GCG Wisconsin Package (Accelrys, San Diego, USA).

To construct the expression plasmids for the recombinant Y472F and Q514G mutants of PAC α F2, pGEX-F2 vectors were point-mutated by site-directed mutagenesis (QuickChange site-directed mutagenesis kit, Stratagene, La Jolla, CA, USA), resulting in pGEX-F2(Y472F) and pGEX-F2(Q514G) for expressions of point-mutated GST-F2 proteins [GST-F2(Y472F) and GST-F2(Q514G)], respectively.

Another construct for expression of recombinant PAC α F2 was made using a T7 RNA polymerase-based overexpression system that added a His-tag to the amino terminus of the protein. A DNA fragment including the multiple cloning site from plasmid pET28a(+) (EMD Biosciences, Darmstadt, Germany) was removed using *Apa*I and *Xho*I and was cloned into the *Apa*I and *Xho*I restriction sites of pET21d(+) (EMD Biosciences) for selection of transformed cells with ampicillin, resulting in plasmid pET21d(28a). Next, the PCR-amplified fragment of F2 was inserted into the multiple cloning site (using *Bam*HI-*Sal*I restriction sites) of pET21d(28a), resulting in recombinant plasmid pET21d(28a)-F2 for expression of the His-tagged F2 protein (6His-F2) (Fig. 1).

To construct the expression plasmids of PAC α F1, the region from Gly48 to His158, which includes the F1 domain, was amplified using the PCR with DNA polymerase (Pyrobest, Takara) and the cloned cDNA encoding PAC α . The PCR-amplified fragments of F1 were cloned into *Bam*HI-*Sal*I restriction sites of pGEX-6P-2 and pET21d(28a), resulting in recombinant plasmids pGEX-F1 and pET21d(28a)-F1 for expressions of the GST-fused F1 protein (GST-F1) and His-tagged F1 protein (6His-F1) (Fig. 1), respectively.

Recombinant EtgPAC1 F2 was overexpressed in *E. coli* using the T7 RNA polymerase-based expression system. The region from Met467 to Thr570 of EtgPAC1, which includes the EtgPAC1 F2 domain, was amplified by PCR using DNA polymerase (Pyrobest, Takara). Forward and reverse primers, 5'-GGGAATTACATATGGCCGGAGGAGGC-3' and 5'-CGTCGACTACGTAGCAGCAGTCACAGAGA-3', were used to amplify the EtgPAC1 F2 coding sequence, adding *Nde*I and *Sal*I restriction sites and a stop codon. A cloned cDNA encoding EtgPAC1 was used as a PCR template. The PCR-amplified fragment was inserted into *Nde*I-*Sal*I restriction sites of pET21d(28a), resulting in recombinant plasmid pET21d(28a)-(EtgPAC1)F2 for expression of the His-tagged EtgPAC1 F2 protein (6His-(EtgPAC1)F2).

Expression and purification of GST-F1, GST-F2, GST-F2(Y472F), and GST-F2(Q514G)

The recombinant plasmids pGEX-F1, pGEX-F2, pGEX-F2(Y472F), and pGEX-F2(Q514G) were separately introduced into *E. coli* strain BL21 (Amersham Bioscience). The cells

were cultured in Luria broth (LB) containing 100 $\mu\text{g ml}^{-1}$ ampicillin. GST-F2 was overexpressed by induction with 5 μM isopropyl- β -D-thiogalactopyranoside (IPTG) at 15 $^{\circ}\text{C}$ for 15 h in darkness. Harvested cells were suspended in phosphate buffered saline, pH 7.4, and broken by ultrasonication (20 kHz, 50 W). The soluble GST-F1, GST-F2, GST-F2(Y472F), and GST-F2(Q514G) in the supernatants after centrifugation (at 10 000 g for 30 min at 4 $^{\circ}\text{C}$) of the sonicates were affinity-purified using GST-binding resin (Glutathione Sepharose 4B, Amersham Bioscience) and elution buffer, 50 mM Tris-HCl, containing 10 mM reduced glutathione, pH 9, as described by the manufacturer.

Purification of GST-cleaved F2

The above described GST-F2 bound to the GST-binding resin was cleaved using a protease (PreScission Protease, Amersham Bioscience) in a cleavage buffer as described by the manufacturer, and the soluble GST-cleaved F2 was then collected as supernatant after centrifugation (at 500 g for 10 min at 4 $^{\circ}\text{C}$).

Expressions, solubilizations, and assemblies of 6His-F1 and 6His-F2

The recombinant plasmids pET21d(28a)-F1 and pET21d(28a)-F2 were introduced into *E. coli* strain BL21(DE3) (EMD Biosciences) and cultured as described above. The cells were cultured in LB containing 100 $\mu\text{g ml}^{-1}$ ampicillin. 6His-F1 and 6His-F2 were overexpressed by induction with 0.5 mM IPTG at 37 $^{\circ}\text{C}$ for 6 h. Almost all of the expressed 6His-F1 and 6His-F2 were present in insoluble inclusion bodies. Harvested cells were suspended in potassium phosphate buffer, pH 7. The cells were broken by ultrasonication. Inclusion bodies were separated from the sonicate by centrifugation at 10 000 g for 30 min at 4 $^{\circ}\text{C}$, and the pellet was resuspended and washed with 50 mM potassium phosphate buffer, pH 7, containing 4% Triton X-100, and finally suspended in 50 mM potassium phosphate buffer, pH 7. An aliquot of the inclusion body suspension, containing 4.2 mg ml^{-1} total protein for 6His-F2, was mixed with 3 parts of 8 M guanidine-HCl solution, resulting in a denatured protein solution.

Protein-refolding of 6His-F2 was performed by rapid manual mixing of an aliquot of the suspension of denatured 6His-F2 solution with 12.5 parts of the refolding buffer: 50 mM potassium phosphate buffer, pH 7, containing 20 μM exogenous flavins, FAD (F-6625, Sigma, St. Louis, MO, USA) or flavin mononucleotide (FMN) (F-8399, Sigma). The assembling efficiencies for 6His-F2 were low when refolding buffers with pH lower than 7 were used. Protein-refolding of 6His-F1 was performed using the refolding buffer containing 20 μM FAD.

The refoldings of denatured 6His-F1 and 6His-F2 were completed by stabilization at *ca.* 24 $^{\circ}\text{C}$ for 20 min in darkness. After the insoluble proteins were removed from the refolded protein solutions by centrifugation at 10 000 g for 30 min at 4 $^{\circ}\text{C}$, purification of 6His-F1 and 6His-F2 was performed using His-tag-binding resin (Talon metal affinity resin, BD Biosciences Clontech, Palo Alto, CA, USA) and elution buffer as described by the manufacturer.

Expression and purification of 6His-(EtgPAC1)F2

The recombinant plasmid pET21d(28a)-(EtgPAC1)F2 was introduced into *E. coli* strain BL21 trxB (DE3) (EMD Biosciences). The cells were cultured in LB containing 100 $\mu\text{g ml}^{-1}$ ampicillin and 25 $\mu\text{g ml}^{-1}$ kanamycin. 6His-(EtgPAC1)F2 was overexpressed by induction with 10 μM IPTG at 15 $^{\circ}\text{C}$ for 15 h. The soluble 6His-(EtgPAC1)F2 was extracted from the cells by ultrasonication and centrifugation at 10 000 g for 30 min at 4 $^{\circ}\text{C}$, and was then purified by affinity chromatography using the metal affinity resin as described by the manufacturer.

F1 and F2 preparations for spectrophotometric analyses

The eluted samples of all the above described recombinant F1 and F2 proteins were concentrated by ultrafiltration (Ultrael YM membranes, Millipore, MA, USA). The buffers in the concentrates were replaced with fresh phosphate buffer, 50 mM sodium phosphate, 300 mM NaCl, pH 7 (BD Biosciences Clontech) for the removal of released flavins using a gel filtration chromatography kit (Biospin 6 Chromatography Columns, Bio-Rad, Hercules, CA, USA). Appropriate protein concentrations of these F1 and F2 samples were adjusted by dilution with phosphate buffer for various spectroscopic measurements. These procedures were performed under dim-red light. The samples were dark-adapted for more than an hour and stored for less than 24 h on ice in darkness until use.

Biochemical analyses

The purity of recombinant F1 and F2 proteins was estimated by SDS-PAGE. Protein assays were performed by the "standard-assay" method (Bio-Rad Protein Assay, Bio-Rad) as described by the manufacturer.

Heating the purified recombinant F1 and F2 solutions at 95 $^{\circ}\text{C}$ for 3 min released flavins from denatured proteins. After cooling, denatured proteins were removed by centrifugation at 12 000 g for 15 min followed by filtration (Microcon YM-3, Millipore). The extracted flavins were examined by thin-layer chromatographic (TLC) analysis using 1-butanol/acetic acid/water (4 : 1 : 5) as solvent, a silicagel plate (Silicagel 70 Plate-Wako, Wako, Osaka, Japan) and mixtures of authentic FAD (F-6625, Sigma), FMN (F-8399, Sigma) and riboflavin (R-4500, Sigma) as markers.

The concentrations of photochemically-active flavin-binding polypeptides (holoproteins) in the recombinant F2 samples for the spectroscopic analyses were estimated based on the concentrations of flavins in the recombinant F2 samples, assuming that the holoproteins bind flavins with a stoichiometry of 1 : 1. The concentrations of flavins in the recombinant F2 samples were estimated by comparing the spectra of the samples denatured by 4.5 M guanidine-HCl with those of 4.5 M guanidine-HCl solutions containing either FAD ($\epsilon = 11.3 \times 10^3 \text{ M}^{-1} \text{ cm}^{-1}$ at 450 nm) or FMN ($\epsilon = 12.5 \times 10^3 \text{ M}^{-1} \text{ cm}^{-1}$ at 445 nm).^{22,23} The suitability of this concentration of guanidine for complete denaturation was confirmed by complete matching of the spectra of the guanidine-denatured protein solution and the pure flavins in the presence of guanidine-HCl.

Spectrophotometric analyses

UV and visible absorption spectra of the flavin-assembled F1 and F2 samples, in darkness or under blue-light illumination, were measured at *ca.* 24 $^{\circ}\text{C}$ using a photodiode array spectrophotometer (model Multispec-1500, Shimadzu, Kyoto, Japan). Irradiation with blue-light was performed at 100 $\mu\text{mol m}^{-2} \text{ s}^{-1}$ using a LED (model NSPB500S, peak wavelength: 465 nm, full width at half maximum, FWHM: 28 nm, Nichia, Tokushima, Japan).

Spectral kinetics was examined using a dual wavelength spectrophotometer (model 557, Hitachi, Tokyo, Japan) by measuring the time evolution of absorbance changes at 502 nm, where the maximum blue light-induced red-shift was observed. The sample (800 μl) in a fluorometer micro-cell (FM20, GL Sciences, Tokyo, Japan) was irradiated with monochromatic blue light (442 nm) generated by a CW HeCd laser system (model 4074-S-B03, Melles Griot, Carlsbad, CA, USA) at right-angles to the measuring beam. The size of the micro-cell was 10 mm in the measuring beam path and 2 mm in inside width for irradiation. To irradiate the whole sample, the laser beam was expanded by a concave lens (20 mm diameter and 40 mm focal length, Sakai Glass, Tokyo, Japan), mounted at the outlet of the laser beam. Maximum photon fluence rate measured by a photon

density meter (PFDM-200LX, Rayon, Tokyo, Japan) with a silicon photodiode (model S1337-66BQ, Hamamatsu Photonics, Hamamatsu, Japan) at the position of the sample (520 mm from the outlet for laser beam) was *ca.* 2 mmol m⁻² s⁻¹. Neutral density filters (Fujitok, Tokyo, Japan) were used to adjust the photon fluence rate. The actinic irradiation was turned on or off by a shutter system (model #0, Copal, Tokyo, Japan) with an electromagnetic controller (Sigma Koki, Tokyo, Japan). Fitting curves were calculated based on measured time evolutions of absorbance changes by the method of least squares using data analysis software (Delta Graph 5.5J, Rockware, Golden, CO, USA).

Results

Flavin composition

Purity of the GST-F2 and GST-cleaved F2 samples was examined by SDS-PAGE (Fig. 2A). Only a small fraction of the expressed GST-F2 (lane 2) was soluble (lane 3). The eluates of GST-F2 (lane 4) and GST-cleaved F2 (lane 5) exhibited single bands, indicating high purity. The flavins bound to the purified GST-cleaved F2 were FAD and FMN with trace amount of riboflavin, as analysed by TLC analysis (Fig. 2B). 4.4 μM GST-cleaved F2 contained 3.6 μM mixture of flavins. The estimated amount of flavin bound to GST-cleaved F2 was 0.8 mol/mol protein.

The insoluble 6His-F2 was refolded into a soluble form and became the major component of the eluates, obtained by affinity chromatography with the metal affinity resin. TLC analysis identified the extracted flavin from each of these eluates to be the same as the flavin contained in each refolding-buffer used (Fig. 2B), suggesting that 6His-F2 binds exogenously added flavins. These FAD- and FMN-binding His-tagged F2 proteins were designated as 6His-F2-FAD and 6His-F2-FMN, respectively. The purity of the 6His-F2 at different times of overexpression and affinity purification after assembly was also examined by SDS-PAGE as shown in Fig. 2C. The eluate from the metal affinity resin also exhibited a single band, indicating sufficiently high purity. Samples of 3.9 μM 6His-F2-FAD and 6His-F2-FMN contained 3.4 μM of FAD and 3.3 μM of FMN, respectively. The protein solutions of 6His-F2-FAD and 6His-F2-FMN contained flavin moieties at ratios 0.87 and 0.85 mol/mol protein, respectively.

As for PACα F1 samples, GST-F1 exhibited a single band (Fig. 2A, lane 6), indicating high purity, and the above described procedure to recover from inclusion bodies yielded

soluble 6His-F1 (Fig. 2C, lane 6). However, no flavins were detected for the PACα F1 samples by TLC analysis (data not shown). This fact was confirmed by the absence of flavin-type absorption in PACα F1 samples (Fig. 3) as described below.

The affinity-purified GST-F2(Y472F), GST-F2(Q514G), and 6His-(EtgPAC1)F2 also showed high purity and contained both FAD and FMN with trace amounts of riboflavin (data not shown).

Absorption spectra and blue-light-induced absorbance changes of the F1 and F2 preparations

The spectrum of dark-adapted GST-F2 (Fig. 3A) exhibited two broad absorption bands, with peaks at 381 and 454 nm, slightly different from those of the prokaryotic BLUF domains (*e.g.*, 365 and 445 nm for AppA,^{6,7} 378 and 443 nm for Slr1694,¹⁵ 383 and 437 nm for Tll0078¹⁶). Dark-adapted GST-F1 did not exhibit such flavin-type broad absorption bands.

The absorption spectra of dark-adapted GST-F2(Y472F) (with peaks at 380 nm and 455 nm), GST-F2(Q514G) (with peaks at 378 nm and 453 nm), and 6His-(EtgPAC1)F2 (with peaks at 377 nm and 452 nm) (Fig. 3B) were similar to those of dark-adapted GST-F2. The absorption spectrum of dark-adapted GST-F2 displayed the light-induced red-shifts, but those of dark-adapted GST-F2(Y472F), GST-F2(Q514G), and 6His-(EtgPAC1)F2 did not.

Dark-adapted 6His-F2-FAD and 6His-F2-FMN showed almost the same absorption spectra as that of GST-cleaved F2 (Fig. 3C). The dark-adapted 6His-F1 did not show the flavin-type two broad absorption bands (Fig. 3C).

As a consequence of the red-shift, the absorbance of GST-F2 and GST-cleaved F2 at 394, 467, and 502 nm underwent significant positive changes, and that at 425, 450, and 481 nm significant negative changes by irradiation with blue light, but absorbance at 550 nm did not (Fig. 3D). The red-shifted spectrum returned in the dark to that of dark-adapted GST-cleaved F2, thus displaying a photocycle. The dark-adapted 6His-F2-FAD and 6His-F2-FMN showed almost the same red-shift in the visible absorption spectra as GST-cleaved F2 (Fig. 3C and 3D). These results are similar to those of the prokaryotic BLUF domains, AppA, Slr1694, and Tll0078, although they display slightly different red-shifts. For example, GST-cleaved F2, 6His-F2-FAD, and 6His-F2-FMN showed the highest absorbance change at 502 nm, whereas AppA, Slr1694, and Tll0078 did so at 495,^{6,7} 488,¹⁸ and 482¹⁶ nm, respectively.

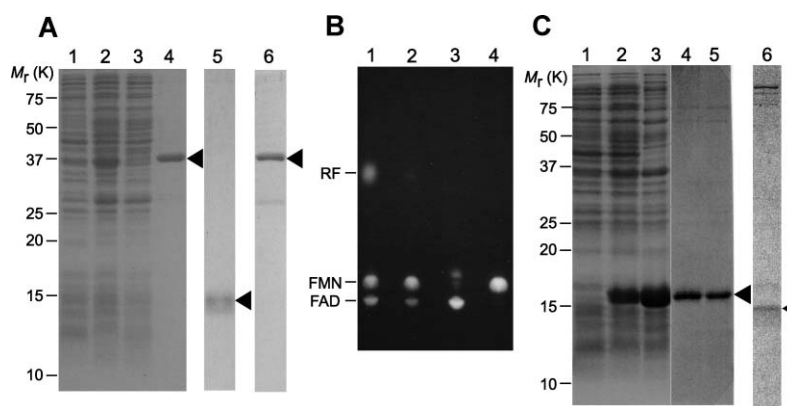


Fig. 2 Purification of recombinant PACα F1 and F2 samples. (A) SDS-PAGE of overexpressed and purified GST-cleaved F2. Lane 1, crude extract of BL21 (pGEX-F2) before induction with IPTG; lane 2, BL21 (pGEX-F2) 15 h after induction; lane 3, supernatant of sonicate; lane 4, affinity-purified GST-F2; lane 5, concentrate of GST-cleaved F2; lane 6, affinity-purified GST-F1. (B) TLC analysis of flavins in the recombinant PACα F2 samples. Lane 1, mixture of authentic FAD, FMN and riboflavin (RF); lane 2, GST-cleaved F2; lane 3, 6His-F2-FAD; lane 4, 6His-F2-FMN. Spots represent fluorescence emissions following illumination with UV-A. (C) SDS-PAGE of overexpressed and purified 6His-F2. Lane 1, crude extract of BL21(DE3) (pET21(28)-F2) before induction; lane 2, BL21(DE3) (pET21(28)-F2) after induction with IPTG; lane 3, inclusion body suspension; lane 4, affinity-purified 6His-F2-FAD; lane 5, affinity-purified 6His-F2-FMN; lane 6, affinity-purified 6His-F1. (A) and (C) were stained with Coomassie Brilliant Blue.

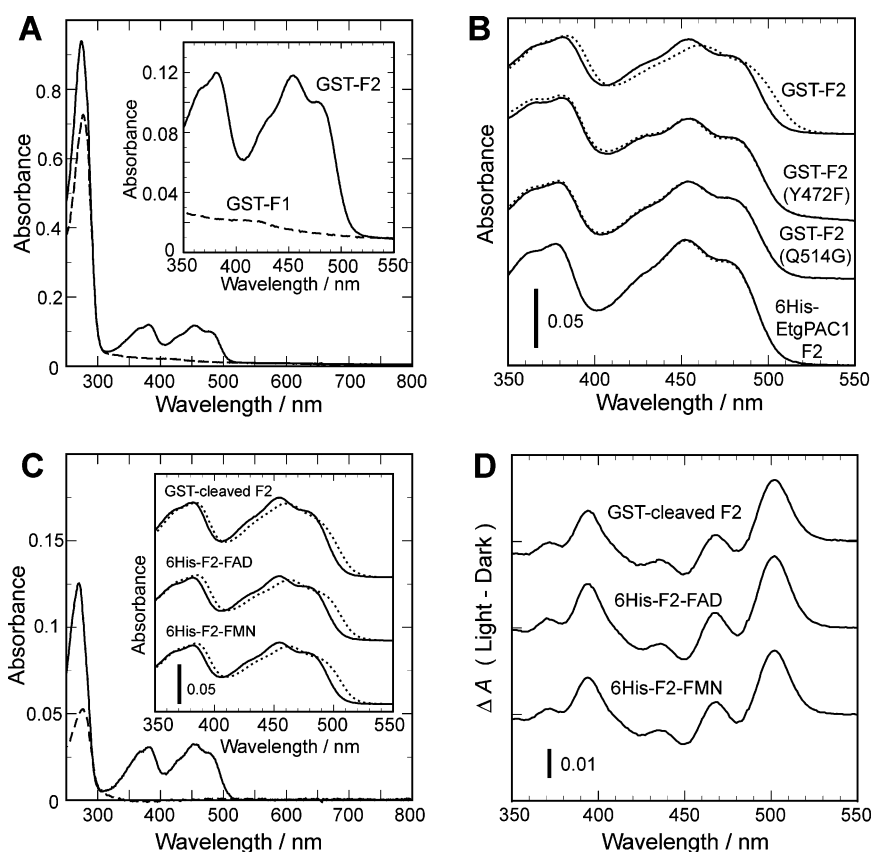


Fig. 3 UV and visible absorption (A, B, and C) and absorption difference (D) spectra of recombinant PAC α F1 and F2 samples. (A) The spectra of dark-adapted GST-F1 (dashed line) and GST-F2 (solid line). Inset shows the magnified spectra of dark-adapted GST-F1 and GST-F2 in the wavelength of 350 to 550 nm. (B) The spectra of dark-adapted and blue-light-irradiated GST-F2, GST-F2(Y472F), GST-F2(Q514G), and 6His-(EtgPAC1)F2. (C) The spectra of dark-adapted 6His-F1 (dashed line) and 6His-F2-FAD (solid line). Inset shows the spectra of dark-adapted and blue-light-irradiated GST-cleaved F2, 6His-F2-FAD, and 6His-F2-FMN. (D) The absorption difference spectra of GST-cleaved F2, 6His-F2-FAD, and 6His-F2-FMN. In (B), inset of (C) and (D), the dark-adapted samples (solid line) were irradiated by a LED (465 nm, FWHM: 28 nm) at a photon fluence rate of 100 $\mu\text{mol m}^{-2} \text{s}^{-1}$. Spectra of light-irradiated samples (dotted line) were acquired at 60 s after the onset of irradiation.

Kinetic characterization of photocycles of different F2 preparations

The time evolutions of absorbance changes at 502 nm, designated as $\Delta A_{502 \text{ nm}}$, are shown in Fig. 4A. $\Delta A_{502 \text{ nm}}$ at various photon fluence rates below 100 $\mu\text{mol m}^{-2} \text{s}^{-1}$, were measured at 25 °C for dark-adapted GST-cleaved F2, 6His-F2-FAD, and 6His-F2-FMN samples with 3.6 μM flavins at estimated molar ratios of 1 : 4 (FAD : FMN) (*cf.* Fig. 2B), 3.4 μM FAD, and 3.3 μM FMN, respectively. Moreover, photocycles were examined on 6His-F2-FAD and 6His-F2-FMN at various concentrations (below 8 μM flavins in these recombinant F2 samples).

The time resolved $\Delta A_{502 \text{ nm}}$ were analyzed by assuming the following simplified photochemical model with a ground state (A) and a signaling state (B) which causes the red-shift of absorption spectrum for the light-reaction of photocycle at room temperature:



where k_1 and k_2 are rate constants. k_1 is given by the equation $k_1 = \Phi \kappa E_{p,o}$, where Φ is the quantum efficiency, κ is the molar absorption cross section and $E_{p,o}$ is the photon fluence rate. In the dark-relaxation phase the formation of B stops, and B returns to A with the rate constant k_2 . This photochemical reaction model gives the simultaneous differential equations for the concentrations of A and B, $d[A]/dt = -k_1[A] + k_2[B]$ and $d[B]/dt = k_1[A] - k_2[B]$. By substituting solutions of these differential equations into equation $\Delta A_{502 \text{ nm}} = \epsilon_A[A] + \epsilon_B[B] -$

$\epsilon_A[A]_0$, the calculated time-dependent values of $\Delta A_{502 \text{ nm}}$ are given by the following equations,

$$\Delta A_{502 \text{ nm}} (\text{light-on}) = \Delta A_{\text{max}} (1 - e^{-k_{\text{on}} t}) \quad (2)$$

$$\Delta A_{502 \text{ nm}} (\text{light-off}) = \Delta A_{\text{max}} e^{-k_{\text{off}} t} \quad (3)$$

where the values of t in equations (2) and (3) are the blue-light irradiation time and the decaying time in darkness, respectively. $[A]_0$ is the initial concentration of flavin-binding protein (A), and given by equation $[A]_0 = [A] + [B]$. ϵ_A and ϵ_B are molar absorption coefficients at 502 nm for A and B, respectively. ΔA_{max} is the saturated (maximum) level in a stationary state of $\Delta A_{502 \text{ nm}}$, k_{on} is the observed rate constant of light-reaction, and k_{off} is the observed rate constant of dark-relaxation. The initial velocity (V_0) is a slope of a tangent line to the time evolution curve of $\Delta A_{502 \text{ nm}}$ at the onset of irradiation and given by equation $V_0 = \Delta A_{\text{max}} k_{\text{on}} \cdot \Delta A_{\text{max}}$, k_{on} , V_0 , and k_{off} are related to the photon fluence rate ($E_{p,o}$) by the following equations,

$$\Delta A_{\text{max}} = \frac{(\epsilon_B - \epsilon_A) \Phi \kappa E_{p,o} [A]_0}{\Phi \kappa E_{p,o} + k_2} \quad (4)$$

$$k_{\text{on}} = \Phi \kappa E_{p,o} + k_2 \quad (5)$$

$$V_0 = (\epsilon_B - \epsilon_A) \Phi \kappa E_{p,o} [A]_0 \quad (6)$$

$$k_{\text{off}} = k_2 \quad (7)$$

Calculated and measured values of $\Delta A_{502 \text{ nm}}$ were in good agreement for all the samples of GST-cleaved F2, 6His-F2-FAD and 6His-F2-FMN (Fig. 4). Fig. 5 shows that these kinetic

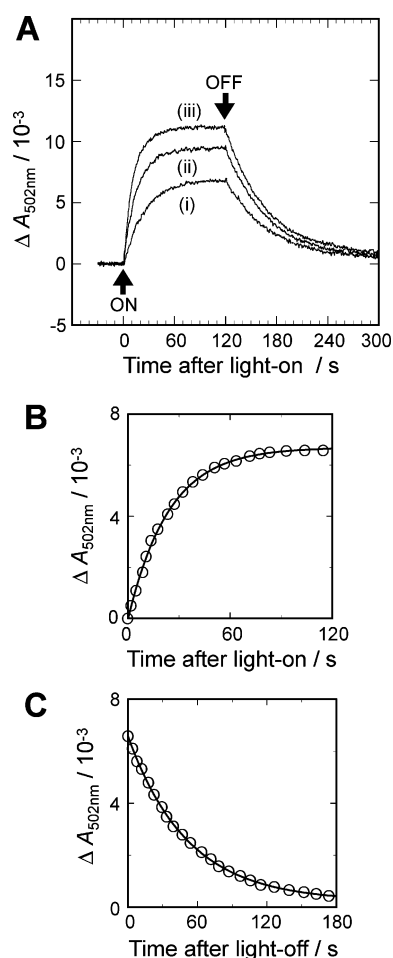


Fig. 4 Light-induced absorption changes of GST-cleaved F2. (A) The time evolutions of $\Delta A_{502\text{nm}}$ were measured at 25 °C using a dual wavelength spectrophotometer under irradiation with 442 nm (generated by a HeCd laser system) at photon fluence rates of 24 (i), 47 (ii), and 90 (iii) $\mu\text{mol m}^{-2} \text{s}^{-1}$, respectively, for GST-cleaved F2, which contained 3.6 μM flavins at an estimated molar ratio of 1 : 4 (FAD : FMN). Arrows indicate timings of turning on and off of irradiation. (B) Calculated curve and plots (circles) of raw data for the photoinduced reaction (i). (C) Calculated curve and plots (circles) of raw data for dark-relaxation on measurement (i).

characteristics of ΔA_{max} , k_{on} , V_0 and k_{off} were in good agreement with eqn (4) to (7), respectively, relating with $E_{\text{p.o}}$ and $[A]_0$. These experimental results for recombinant PAC α F2 support the validity of the simplified photochemical model (1).

From the plots of k_{off} (Fig. 5D), the values of half-life in dark-relaxation, given by equation $t_{1/2\text{off}} = \ln 2 k_{\text{off}}^{-1}$, for GST-cleaved F2, 6His-F2-FAD, and 6His-F2-FMN were determined to be 34, 44, and 40 s, respectively. From the plots of k_{on} (Fig. 5B), the values of $\Phi\kappa$, were determined. The values of κ at 442 nm were estimated by equation $\kappa = 2.303 \epsilon_{442}$, where ϵ_{442} is the molar absorption coefficient at 442 nm for dark-adapted samples. The values of ϵ_{442} for GST-cleaved F2, 6His-F2-FAD, and 6His-F2-FMN were 10.9×10^3 , 10.4×10^3 , and $10.8 \times 10^3 \text{ M}^{-1} \text{ cm}^{-1}$, respectively. With these values, the values of Φ for GST-cleaved F2, 6His-F2-FAD, and 6His-F2-FMN were calculated to be 0.32, 0.28, and 0.28, respectively. These values are similar to those for AppA (0.24)¹³ and Tll0078 (0.29).¹⁶ From the plots of ΔA_{max} shown in Fig. 5A, or those of V_0 shown in Fig. 5C, the values of $(\epsilon_{\text{B}} - \epsilon_{\text{A}}) [A]_0$ were determined. The estimated values of ϵ_{A} were 2.0×10^3 , 2.1×10^3 , and $2.1 \times 10^3 \text{ M}^{-1} \text{ cm}^{-1}$ for the dark-adapted GST-cleaved F2, 6His-F2-FAD, and 6His-F2-FMN. With these values, ϵ_{B} for GST-cleaved F2, 6His-F2-FAD, and 6His-F2-FMN were calculated to be 6.0×10^3 , 5.7×10^3 , and $5.7 \times 10^3 \text{ M}^{-1} \text{ cm}^{-1}$, respectively.

Discussion

Selectivity in flavin-binding by F2 and prokaryotic BLUF domains

Purified GST-cleaved F2 bound not only FAD but also FMN and riboflavin although native PAC seems to bind only FAD.^{1,2} At first glance, this may indicate that extracted FMN was a decomposition product of FAD initially bound to recombinant F2 during expression and/or purification. Taken together, however, the facts that the ultracentrifuged supernatant of boiled homogenate of the cell contained FAD and FMN (data not shown) and that 6His-F2 could bind either FAD or FMN by assembly as described above, it is more probable that the extracted FMN was bound to recombinant F2 from the beginning of expression in *E. coli*.

Thus, recombinant F2 can bind either FAD or FMN. A possible interpretation for the exclusive FAD binding of the native PAC protein might be that only native PAC with FAD could fold into the correct (e.g., the $\alpha_2\beta_2$ heterotetramer) protein structure.

The spectral characteristics of the assembled 6His-F2 binding FAD and 6His-F2 binding FMN were similar to those of GST-cleaved F2. The rate constants of light-reaction and dark-relaxation of the 6His-F2-FAD and 6His-F2-FMN are slightly lower than those of GST-cleaved F2.

The kinetic characteristics of photocycles of 6His-F2-FAD and 6His-F2-FMN were nearly the same. This fact suggests that the adenine ring of FAD is not essential in the photochemical reaction of the photocycle, at least in recombinant PAC α F2. The rate constants of light-reaction and dark-relaxation of the former are just slightly smaller than those of the latter. Similarly, it was found that the rate constants of the light-reaction and dark-relaxation of the assembled BLUF domain of AppA binding FAD are smaller than those of the one binding FMN.¹¹ Such slight differences in the kinetic characteristics of the photocycle between FAD-binding and FMN-binding BLUF domains should then result from some factor other than the isoalloxazine ring (e.g., the adenine ring).

Differences in the two BLUF domains, F1 and F2, of PAC

The interchanged F1 in place of the BLUF domain of AppA mediated light-dependent gene expression in *R. sphaeroides*.²⁴ This fact suggests that the mechanisms of photosensing of eukaryotic and prokaryotic BLUF domains are essentially the same even though they are involved in different types of photoreactions, i.e. photomovements through activation of the adenylyl cyclase domain in the former and gene expression or photomovement control in the latter. This report also indicates that F1 can play a role as a blue-light sensing domain *in vivo* at least when heterologously expressed in *R. sphaeroides*. It is assumed that PAC α F1 binds FAD, because PAC α F1 and PAC α F2 have similar homologous regions. Strangely enough, however, recombinant PAC α F1 samples (the region from Gly48 to His158 of PAC α) did not bind flavins (Fig. 3A and 3C), although we could obtain sufficient amount of the soluble recombinant PAC α F1 by heterologous expression with fused GST in *E. coli* (BL21) and the above described procedure to recover from inclusion bodies gave the soluble recombinant PAC α F1 (6His-F1). The reason why no flavins bind to the recombinant PAC α F1 samples is not yet clear.

It is noteworthy that in phototropin, another flavin-based blue-light sensor that contains two flavin-binding domains (LOV1 and LOV2), phot1 LOV2 exhibits a higher photosensitivity and plays a more important role in the physiological response than LOV1 in phot1.²⁵ The quantum efficiencies of phot1 LOV2 are 10-fold higher [0.44 (oat), 0.34 (*Arabidopsis*), 0.30 (rice)] than those of phot1 LOV1 [0.045 (oat), 0.035 (*Arabidopsis*), 0.026 (rice)] of higher plants.^{26,27} A recent report suggests an interaction between *Chlamydomonas reinhardtii* phototropin

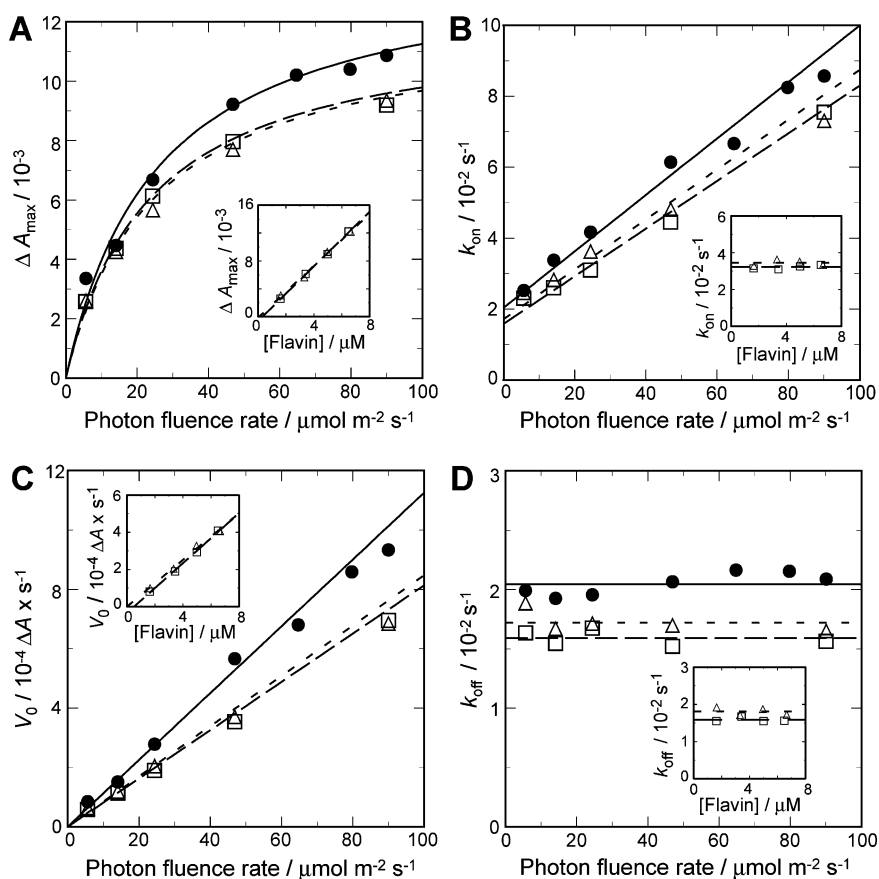


Fig. 5 Kinetic characteristics of photocycle *versus* photon fluence rate for GST-cleaved F2 (—●—), 6His-F2-FAD (—□—), and 6His-F2-FMN (---△---). (A) Maximum $\Delta A_{502\text{nm}}$ (ΔA_{max}). (B) Observed rate constant (k_{on}) upon irradiation. (C) Initial velocities (V_0). (D) Observed rate constant (k_{off}) during dark-relaxation. Kinetic values were determined by exponential curve fitting of the measured time evolutions of $\Delta A_{502\text{nm}}$ at 25 °C upon irradiation at 442 nm, at various photon fluence rates below 100 $\mu\text{mol m}^{-2} \text{s}^{-1}$ for dark-adapted GST-cleaved F2, 6His-F2-FAD, and 6His-F2-FMN samples, with 3.6 μM flavins with estimated molar ratios of 1 : 4 (FAD : FMN), 3.4 μM FAD, and 3.3 μM FMN, respectively. Kinetic values in insets were determined for samples with various protein concentrations for 6His-F2-FAD and 6His-F2-FMN. The horizontal axes of the insets show the concentration of flavins in recombinant F2 samples. Irradiation was performed at 24 $\mu\text{mol m}^{-2} \text{s}^{-1}$.

LOV1 and LOV2 domains in the photocycle, indicating that decay behavior of photoproducts in the coexisting domains is different from that in individual domains.²⁸ In this context, the photocycle characteristics of F1 and F2 should be compared both separately and jointly. Because of this, it is not clear which domains of F1 and F2 play more important roles in photoactivation of PAC.

Comparison of photocycling characteristics of F2 preparations with those of prokaryotic BLUF domains

The recombinant Y472F and Q514G mutants of PAC α F2 did not show a light-induced red-shift of absorption (Fig. 3B), similarly to the Y21F mutant of AppA and the Y8F mutant of Slr1694, and Q50A of Tll0078. Recombinant EtpAC1 F2, although having the tyrosine residue, did not show the spectral red-shift (Fig. 3B). These facts indicate that the tyrosine residue and the glutamine residue conserved in PAC play essential roles in the photocycle in recombinant PAC α F2, similarly to prokaryotic BLUF domains.

As described above, the eukaryotic BLUF domain of PAC showed essentially the same photocycle as prokaryotic BLUF domains in the time windows studied, from milliseconds to minutes. The values of $t_{1/2\text{off}}$ of 34–44 s at 25 °C for recombinant PAC α F2 is closer to that of cyanobacterial BLUF domains [Slr1694 (~11 s)¹⁴ and Tll0078 (~3.5 s)¹⁴], rather than that of the purple bacterial BLUF domain [AppA (900 s)^{6,7}]. Taking into account that not only PAC but also Slr1694 and Tll0078 probably mediate photomovements, their relatively short recovery times may be needed for maintenance of the photomovement responses in contrast to the gene expression control mediated

by the latter (AppA), which is a relatively slow response. The recently reported rapid formation of the signaling state (within 10 ns)^{13,16} in contrast with the longer and diverse lifetime (*i.e.* $t_{1/2\text{off}}$ of several seconds to 900 s) of prokaryotic BLUF domains, raises the question about the mechanism by which the diversity of time parameters are caused. In this regard it is noteworthy that an extracted PAC solution responded to repetitive blue light pulses of various durations (down to 50 ms) with equal efficiencies.²⁹ The molecular mechanism of putative interaction between the BLUF domain(s) and the adenylyl cyclase domains in the photoactivation of PAC constitutes a challenging subject for future studies.

Acknowledgements

We are grateful to Dr Shinji Masuda and Mr Takanori Nakamura for valuable advice, and Ms Yumiko Makino for spectroscopical support. We acknowledge Drs Chris Bowler and Silvia Braslavsky for reading the manuscript. This work was supported in part by a Grant-in-Aid for Scientific Research from the Ministry of Education, Science, Sports and Culture of Japan (15207006 to MW and 17657018 to AM) and the Foundation for Promotion of Photosciences and Phototechnologies. S. Ito acknowledges National Institute for Basic Biology, for a fellowship during part of this study.

References

- 1 M. Iseki, S. Matsunaga, A. Murakami, K. Ohno, K. Shiga, K. Yoshida, M. Sugai, T. Takahashi, T. Hori and M. Watanabe, A blue-light-activated adenylyl cyclase mediates photoavoidance in *Euglena gracilis*, *Nature*, 2002, **415**, 1047–1051.

- 2 M. Watanabe and M. Iseki, Discovery and characterization of photoactivated adenylyl cyclase (PAC), a novel blue-light receptor flavoprotein, from *Euglena gracilis* in *Handbook of Photosensory Receptors*, ed. W. R. Briggs and J. L. Spudich, Wiley-VCH Verlag GmbH & Co. KGaA, Weinheim, 2005, pp. 447–460.
- 3 M. Gomelsky and G. Klug, BLUF: a novel FAD-binding domain involved in sensory transduction in microorganisms, *Trends Biochem. Sci.*, 2002, **27**, 497–500.
- 4 Y. Koumura, T. Suzuki, S. Yoshikawa, M. Watanabe and M. Iseki, The origin of photoactivated adenylyl cyclase (PAC), the *Euglena* blue-light receptor: phylogenetic analysis of orthologues of PAC subunits from several euglenoids and trypanosome-type adenylyl cyclase from *Euglena gracilis*, *Photochem. Photobiol. Sci.*, 2004, **3**, 580–586.
- 5 M. Gomelsky and S. Kaplan, AppA, a redox regulator of photosystem formation in *Rhodobacter sphaeroides* 2.4.1, is a flavoprotein, *J. Biol. Chem.*, 1998, **52**, 35319–35325.
- 6 S. Masuda and C. E. Bauer, AppA is a blue light photoreceptor that antirepresses photosynthesis gene expression in *Rhodobacter sphaeroides*, *Cell*, 2002, **110**, 613–623.
- 7 B. J. Kraft, S. Masuda, J. Kikuchi, V. Dragnea, G. Tollin, J. M. Zaleski and Carl E. Bauer, Spectroscopic and mutational analysis of the blue-light photoreceptor AppA: A novel photocycle involving flavin stacking with an aromatic amino acid, *Biochemistry*, 2003, **42**, 6726–6734.
- 8 S. Masuda and C. E. Bauer, The antirepressor AppA uses the novel flavin-binding BLUF domain as a blue-light-absorbing photoreceptor to control photosystem synthesis in *Handbook of Photosensory Receptors*, ed. W. R. Briggs and J. L. Spudich, Wiley-VCH Verlag GmbH & Co. KGaA, Weinheim, 2005, pp. 433–445.
- 9 W. Laan, M. A. van der Horst, I. H. van Stokkum and K. J. Hellingwerf, Initial characterization of the primary photochemistry of AppA, a blue-light-using flavin adenine dinucleotide-domain containing transcriptional antirepressor protein from *Rhodobacter sphaeroides*: a key role for reversible intramolecular proton transfer from the flavin adenine dinucleotide chromophore to a conserved tyrosine?, *Photochem. Photobiol.*, 2003, **78**, 290–297.
- 10 M. A. van der Horst and K. J. Hellingwerf, Photoreceptor proteins, “star actors of modern times”: a review of the functional dynamics in the structure of representative members of six different photoreceptor families, *Acc. Chem. Res.*, 2004, **37**, 13–20.
- 11 W. Laan, T. Bednarz, J. Heberle and K. J. Hellingwerf, Chromophore composition of a heterologously expressed BLUF-domain, *Photochem. Photobiol. Sci.*, 2004, **3**, 1011–1016.
- 12 S. Masuda, K. Hasegawa and T. Ono, Light-induced structural changes of apoprotein and chromophore in the sensor of blue light using FAD (BLUF) domain of AppA for a signaling state, *Biochemistry*, 2005, **44**, 1215–1224.
- 13 M. Gauden, S. Yermenko, W. Laan, I. H. M. van Stokkum, J. A. Ihalainen, R. van Grondelle, K. J. Hellingwerf and J. T. M. Kennis, Photocycle of the flavin-binding photoreceptor AppA, a bacterial transcriptional antirepressor of photosynthesis genes, *Biochemistry*, 2005, **44**, 3653–3662.
- 14 K. Okajima, S. Yoshihara, Y. Fukushima, X. Geng, M. Katayama, S.-I. Higashi, M. Watanabe, S. Sato, S. Tabata, Y. Shibata, S. Itoh and M. Ikeuchi, Biochemical and functional characterization of BLUF-type flavin-binding proteins of two species of cyanobacteria, *J. Biochem.*, 2005, **137**, 741–750.
- 15 S. Masuda, K. Hasegawa, A. Ishii and T. Ono, Light-Induced structural changes in a putative blue-light receptor with a novel FAD binding fold sensor of blue-light using FAD (BLUF); Slr1694 of *Synechocystis* sp. PCC6803, *Biochemistry*, 2004, **43**, 5304–5313.
- 16 Y. Fukushima, K. Okajima, Y. Shibata, M. Ikeuchi and S. Itoh, Primary intermediate in the photocycle of a blue-light sensory BLUF FAD-protein, Tll0078, of *Thermosynechococcus elongatus* BP-1, *Biochemistry*, 2005, **44**, 5149–5158.
- 17 K. Hasegawa, S. Masuda and T. Ono, Spectroscopic analysis of the dark relaxation process of a photocycle in a sensor of blue light using FAD (BLUF) protein Slr1694 of the cyanobacterium *Synechocystis* sp. PCC6803, *Plant Cell Physiol.*, 2005, **46**, 136–146.
- 18 K. Hasegawa, S. Masuda and T. Ono, Structural intermediate in the photocycle of BLUF (sensor of blue light using FAD) protein Slr1694 in a cyanobacterium *Synechocystis* sp. PCC6803, *Biochemistry*, 2004, **43**, 14979–14986.
- 19 A. Kita, K. Okajima, Y. Morimoto, M. Ikeuchi and K. Miki, Structure of a Cyanobacterial BLUF Protein, Tll0078, Containing a novel FAD-binding blue light sensor domain, *J. Mol. Biol.*, 2005, **349**, 1–9.
- 20 S. Anderson, V. Dragnea, S. Masuda, J. Ybe, K. Moffat and C. Bauer, Structure of a novel photoreceptor, the BLUF domain of AppA from *Rhodobacter sphaeroides*, *Biochemistry*, 2005, **44**, 7998–8005.
- 21 M. Watanabe, M. Iseki, S. Ito and A. Murakami, in: Abstracts to the 14th International Congress on Photobiology, June 10 to 15, Jeju, Korea, 2004, abstract S12-07, P. 107.
- 22 C. Walsh, J. Fisher, R. Spencer, D. W. Graham, W. T. Ashton, J. E. Brown, R. D. Brown and E. F. Rogers, Chemical and enzymatic properties of riboflavin analogues, *Biochemistry*, 1978, **17**, 1942–1951.
- 23 C. Thorpe, R. G. Mathews and C. H. Williams, Acyl-coenzyme A dehydrogenase from pig kidney: purification and properties, *Biochemistry*, 1979, **18**, 331–337.
- 24 Y. Han, S. Braatsch, L. Osterloh and G. Klug, A eukaryotic BLUF domain mediates light-dependent gene expression in the purple bacterium *Rhodobacter sphaeroides* 2.4.1, *Proc. Natl. Acad. Sci. USA*, 2004, **101**, 12306–12311.
- 25 J. M. Christie and W. R. Briggs, Blue light sensing and signaling by the phototropins in *Handbook of Photosensory Receptors*, ed. W. R. Briggs and J. L. Spudich, Wiley-VCH Verlag GmbH & Co. KGaA, Weinheim, 2005, pp. 277–303.
- 26 M. Salomon, J. M. Christie, E. Knieb, U. Lempert and W. R. Briggs, Photochemical and mutational analysis of the FMN-binding domains of the plant blue light receptor, phototropin, *Biochemistry*, 2000, **39**, 9401–9410.
- 27 M. Kasahara, T. E. Swartz, M. A. Olney, A. Onodera, N. Mochizuki, H. Fukuzawa, E. Asamizu, S. Tabata, H. Kanegae, M. Takano, J. M. Christie, A. Nagatani and W. R. Briggs, Photochemical properties of the flavin mononucleotide-binding domains of the phototropins from *Arabidopsis*, rice, and *Chlamydomonas reinhardtii*, *Plant Physiol.*, 2002, **129**, 762–773.
- 28 H. Guo, T. Kottke, P. Hegemann and B. Dick, The Phot LOV2 domain and its interaction with LOV1, *Biophys. J.*, 2005, **89**, 402–412.
- 29 S. Yoshikawa, T. Suzuki, M. Watanabe and M. Iseki, Kinetic analysis of the activation of photoactivated adenylyl cyclase (PAC), a blue-light receptor for photomovements of *Euglena*, *Photochem. Photobiol. Sci.*, 2005, DOI: 10.1039/b417212d.